J. Membrane Biol. 60, 199–209 (1981)

The Journal of
Membrane Biology

The Effect of Electrical Gradients on Current Fluctuations and Impedance Recorded from *Necturus* Gallbladder

Heinz Gögelein* and Willy Van Driessche**

Laboratorium voor Fysiologie, KUL, Campus Gasthuisberg, B-3000 Leuven, Belgium

Summary. Transepithelial current fluctuations were recorded in *Necturus* gallbladder, clamped at negative as well as positive potentials up to 64 mV. With NaCl-Ringer's (+10 mM TAP) on both sides a mucosa-negative potential enhanced the relaxation noise component, present at zero potential, and produced peaking in the power spectrum at potentials above −36 mV. Concomitantly at these potentials an inductive as well as a capacitive low-frequency feature appeared in the impedance locus. Clamping at positive potentials of 18 mV suppressed the relaxation noise component. At potentials above 51 mV the spectral values increased predominantly at low frequencies. In this case the power spectrum showed only a $1/f^{\alpha}$ noise component. The experiments confirm the previous finding that a K^+ efflux through fluctuating apical K^+ channels exists under normal conditions. With serosal KCl-Ringer's the initial Lorentzian component was enhanced at negative but suppressed at positive potentials. The increase at negative potentials was less pronounced than in experiments with NaCl-Ringer's on both sides, indicating saturation of the fluctuating K^+ current component. With mucosal KCl-Ringer's a negative potential depressed the initial relaxation noise component, whereas it was enhanced at +18 mV clamp potential. In the latter case an additional Lorentzian component became apparent at higher frequencies. At potentials of 36 mV and above the low-frequency Lorentzian disappeared whereas the corner frequency of the high-frequency component increased. The latter experiments demonstrate that the relaxation noise component in *Necturus* gallbladder consists of two superimposed Lorentzians. As the relaxation times of these two components behave differently under an electrical field, there may exist two different types of K^+ channels. It is demonstrated that peaking in the plateau of power spectra can be explained by frequency-dependent attenuation effects, caused by a polarization impedance.

Key words: *Necturus*, gallbladder, potassium, impedance, noise analysis, apical membrane, voltage

In voltage-clamped gallbladders a relaxation noise component was observed which was strongly dependent on the serosal as well as mucosal K^+ concentration (Van Driessche & Gögelein, 1978; Gögelein & Van Driessche, 1981). The plateau value of the Lorentzian noise component increased gradually with increasing serosal K^+ concentration. However, the relaxation noise was abolished when mucosal K^+ was raised to 36 mM, but it reappeared at higher mucosal K^+ concentrations. The Lorentzian noise component disappeared when 5 mM tetraethylammonium (TEA^+) was added to the mucosal solution and its plateau was reduced after application of 2, 4, 6-triaminopyrimidine (TAP^+). It was concluded that these fluctuations are due to K^+ flow through channels in the apical membrane with open-close kinetics. In the absence of a transepithelial electrochemical gradient the driving force for this K^+ movement is assumed to be due to the intracellular K^+ activity, which is higher than expected for a passive distribution (Zeuthen, 1978; Reuss & Weinman, 1979). As the fluctuations were affected by transepithelial K^+ gradients, they should also be influenced by electrical gradients. If a pore model with simple open-close kinetics is assumed, the plateau value of the power spectrum is proportional to the square of the single-pore current (Verveen & de Felice, 1974; Lindemann & Van Driessche, 1977). Under the assumption that all equivalent resistances of the preparation remain constant, changes in the single-channel current should

* *Present address:* Max-Planck-Institut für Biophysik, Kennedy-Allee 70, D-6000 Frankfurt 70, Germany.

** *To whom reprint requests should be addressed.*

0022-2631/81/0060-0199 $02.20

be proportional to changes in the transepithelial potential V_t. This means that the plateau value should depend on the square of V_t. Consequently, under control conditions (NaCl-Ringer's both sides) the relaxation noise component should increase at mucosa-negative but decrease at mucosa-positive potentials. In order to test this assumption we recorded current fluctuations when the epithelium was clamped at different potentials. Under these conditions the effect of the transepithelial d-c current on the electrical parameters of the preparation must be taken into account. It was reported that transmural d-c pulses produce time-dependent voltage transients in the gallbladder epithelium which are due to polarization of emf's (Wedner & Diamond, 1969; Frömter, 1972; Bindslev, Tormey & Wright, 1974; Reuss & Finn, 1977). In frog gallbladder Bindslev et al. (1974) reported the half-times of build-up and decay of these potentials to be in the order of seconds. This time course can be described by an equivalent parallel RC combination in series with the equivalent impedance of the epithelium. Model calculations showed that the transepithelially recorded fluctuations in current, arising from apical K^+ conductance fluctuations, are attenuated by such polarization impedances (Van Driessche & Gögelein, 1980). In this case the calculations predict 'peaking' in the power spectrum. It will be shown in this study that peaking in the power spectrum appears in conjunction with a capacitive LF feature in the impedance locus, being due to polarization phenomena.

Materials and Methods

The experimental techniques of preparing the tissue, the electrical set-up and analysis of the noise data were as described previously Gögelein & Van Driessche, 1981; Van Driessche & Zeiske, 1980*a*, *b*). The Ringer's solution under control conditions (NaCl-Ringer's) had the following composition (in mM): 109 NaCl, 2.5 KCl, 0.9 $CaCl_2$ and 2.4 $NaHCO_3$, pH = 8.4, when gassed with air. In order to reduce low-frequency (LF) noise and to obtain power spectra, which can be fitted by Lorentzians, 10 mM 2, 4, 6-triaminopyrimidine (TAP) was present on both sides, if not otherwise stated. In the presence of TAP^+ the pH was adjusted to 6 by addition of HCl. With NaCl-Ringer's on both sides current fluctuations were recorded when the epithelium was clamped at zero potential. In order to prevent electrical current flow across the tissue with KCl-Ringer's on one side, control measurements were performed by clamping at the biionic potential (not corrected for liquid junction potentials). The transepithelial clamp voltage could be adjusted by applying a d-c voltage to the command input of the feedback amplifier (*see* Fig. 1 in Van Driessche and Lindemann, 1978). The clamp potential was raised gradually at discrete steps between 0 and 64 mV. Recordings were only started when the d-c current had reached a steady value (5–10 min). In a few experiments voltage noise was recorded under current-clamp conditions immediately after the measurement of current noise. In both cases the transepithelial d-c voltage was adjusted to the same value.

Electrical Set-up and Methods of Impedance Analysis

Method 1. The electrical impedance of the epithelium could be recorded in two different ways. With the first method the transepithelial potential and current signals were monitored with the voltage-clamp system, used for noise measurements. Binary noise sequences from a pseudo-random noise generator (Hewlett Packard, 3722A) were applied to the command input of the feedback amplifier (*see* Fig. 1 in Van Driessche and Lindemann, 1978). The pulse height, arising across the epithelium, was 3 mV. The sequence length of the pseudo-random noise signal was 2047, being one less than the number of data points in one analyzed spectrum. The noise generator was driven by external clock pulses, which were synchronized with those used to sample the current and voltage signals. Using this procedure, the frequencies contained in the command signal, as well as in the voltage and current signals, coincide almost exactly with those analyzed by Fourier Transformation. After passing through low-pass filters (Rockland 852) the current and voltage signals were sampled simultaneously with two sample-and-hold amplifiers. Cross-power spectra between current and voltage signals and auto power spectra of the current signals were calculated by Fast Fourier Transformation (Decus 179). The impedance function was obtained by division of the mean cross-power spectrum by the mean auto power spectrum calculated from 5 records. Current and voltage signals were digitized at intervals of 2 and 0.2 msec. The displayed impedance loci consist of a superposition of these two impedance functions. Because of phase shifts between the current and voltage signals at higher frequencies, caused by the amplifiers, data points above 63 Hz in the low-frequency spectrum and above 632 Hz in the high-frequency spectrum were not taken into account for further analysis. The method described for impedance measurement had the advantage that the impedance function could be recorded directly after the noise measurement without disconnecting the clamp circuit. However, at frequencies above 650 Hz the phase shift between the voltage and current signals, caused by the amplifiers, became more than 2.7 degrees. Therefore a separate set-up was used to record impedance functions up to 6323 Hz.

Method 2. In this method the pulses of the pseudo-random noise generator were converted to a signal of constant current type (pulse height 4 μA) by passing a resistance of 200 kΩ. The current signal was measured with a current-voltage converter (Analog Devices, AD 528), having a feedback resistance of 10 kΩ. The voltage signal was recorded with a differential amplifier (AD 318), having a gain of 10. Both the current and voltage signals were amplified before they were analyzed in a similar way as described for Method 1.

The epithelium of the *Necturus* gallbladder can be represented by the equivalent network, depicted in Fig. 1*a* (Schifferdecker & Frömter, 1978). As the time constants of the apical and basolateral membranes are comparable and as the shunt resistance R_p is low (Schifferdecker & Frömter, 1978) the impedance function yields a circular arc on the impedance locus (Gögelein, Hegel & Weskamp, 1975; Schifferdecker & Frömter, 1978). The center of this semicircle lies slightly above the real axis. This could be due to the existence of distributed time constants, associated with the intercellular space, as demonstrated in a tight epithelium (Clausen, Lewis & Diamond, 1979). The impedance functions were plotted as impedance loci and fitted by a circular arc, using a nonlinear least-squares fitting procedure. Data points in the high- and low-frequency region could be excluded. The parameters obtained from fits of impedance functions of the same preparation, measured with Method 1 and Method 2 were not significantly different. A circular arc with 'depressed' center can be described by the equation (Cole & Cole, 1941):

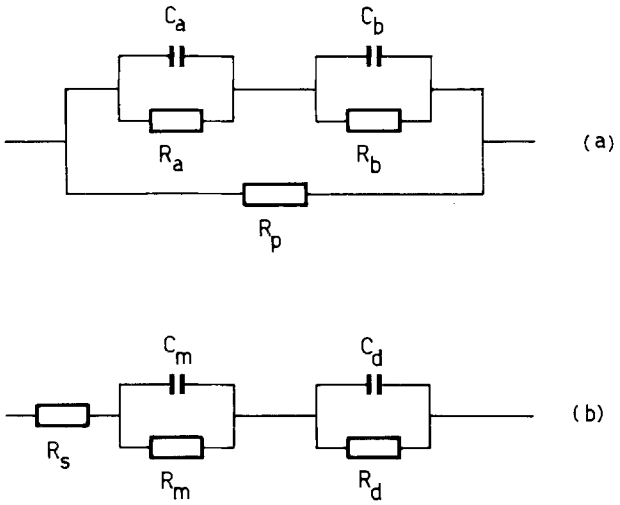

Fig. 1. Equivalent electrical circuits representing electrical properties of the *Necturus* gallbladder. (*a*) Lumped network representing the epithelium in the absence of a polarization impedance. R_a and C_a represent the resistance and capacitance of the apical membrane, R_b and C_b those of the basolateral membrane. R_p represents the paracellular shunt resistance. (*b*) In this circuit the $R_m C_m$ network is a simplified equivalent representation of the epithelial network, shown in (*a*). The $R_d C_d$ combination represents a polarization impedance. R_s represents the resistance of the subserosal layer as well as the resistance of the Ringer's solution between the voltage electrodes

$$Z = R_s + R_m/(1 + (j\omega R_m C_m)^{1-\alpha}) \tag{1}$$

where R_m represents the equivalent parallel resistance, C_m the equivalent parallel capacitance and R_s the resistance in series with this RC network. The angle $\alpha = 2\varphi/\pi$, where φ is the angle between the real axis and a straight line, connecting the center of the semicircle with its intersections with the real axis. The real and imaginary parts of Eq. (1) are given by:

$$Re(Z) = R_s + R_m \cdot (1 + (\omega R_m C_m)^{1-\alpha} \cdot \sin(\alpha\pi/2))/N \tag{2}$$

$$Im(Z) = -R_m \cdot (\omega R_m C_m)^{1-\alpha} \cdot \cos(\alpha\pi/2)/N \tag{3}$$

where

$$N = 1 + 2(\omega R_m C_m)^{1-\alpha} \cdot \sin(\alpha\pi/2) + (\omega R_m C_m)^{2(1-\alpha)}.$$

The resistance R_s is given by the section on the real axis between the origin and the left intercept with the semicircle. R_m is determined by the distance between the intercepts of the semicircle with the real axis. The capacitance C_m was calculated at the discrete frequency point where:

$$Re(Z) - R_s = -Im(Z). \tag{4}$$

Substituting Eqs. (2) and (3) into (4) yields:

$$C_m = \exp(\ln((\cos(\alpha\pi/2) - \sin(\alpha\pi/2))^{-1})/(1-\alpha))/(\omega R_m). \tag{5}$$

The series resistance R_{se}, which is assumed to be due to the subserosal layer of smooth muscles and connective tissue, is given by the difference of R_s and the resistance of the bathing solution between both voltage electrodes. Under control conditions R_{se} was about $12\,\Omega cm^2$ in *Necturus* gallbladder. The total transepithelial resistance R_t is equal to the sum of R_m and R_{se}.

If a capacitive low-frequency feature overlapped significantly with the circular arc of the epithelium, the function

$$Z = R_s + \frac{R_m}{1 + j\omega R_m C_m} + \frac{R_d}{1 + j\omega R_d C_d} \tag{6}$$

was fitted to the data points with a method of nonlinear least squares. Eq. (6) describes a network composed of two RC circuits being in series to the resistance R_s (*see* Fig. 1*b*). It is assumed that the RC network with smaller time constant represents electrical properties inherent to the epithelium, whereas the LF component represents a polarization impedance. In the fitting procedure the parameters R_s, R_m, C_m, R_d and C_d were determined directly by the computer program. This method, however, assumes that the impedance functions with two time constants can be described by a series combination of two ideal RC networks. This may explain the systematic deviations between the data points and the fitted curve observed in some experiments.

Potentials are referred to the serosal side. Errors are presented as standard deviations of the mean.

Results

Impedance Measurements with NaCl-Ringer's on Both Sides

The impedance function of a *Necturus* gallbladder recorded with NaCl-Ringer's on both sides could be fitted by a semicircle with its center situated slightly above the real axis. These results are in good agreement with previous observations (Gögelein et al., 1975; Schifferdecker & Frömter, 1978). Clamping the epithelium at mucosa-negative potentials increased the radius of the circular arc (Fig. 2*a*). With increasing negativity the data points departed from a semicircle in the low- as well as high-frequency range. These points were excluded from the fitting procedure. Mean values of R_m, C_m and φ, obtained at different transepithelial potentials are shown in Fig. 3. At all potentials C_m did not change significantly, whereas φ decreased at negative potentials. With increasing negativity the data points in the LF region of the impedance locus were bent to the left, as expected from an inductive element, and in addition, a capacitive element was indicated (Fig. 2*a*). However, the data points in the LF region could not be fitted by a semicircle. Mucosa-positive potentials did not cause appreciable deviations of the data points from a semicircle (Fig. 2*b*). Fig. 3 demonstrates that R_m decreased at $V = 18$ mV but increased slightly at higher potentials.

Fluctuation Analysis with NaCl-Ringer's on Both Sides

Voltage-clamped ($V = 0$) *Necturus* gallbladders, having NaCl-Ringer's + 10 mM TAP on both sides, yielded, in 44% of all cases, Lorentzian noise components. As discussed in the preceding paper

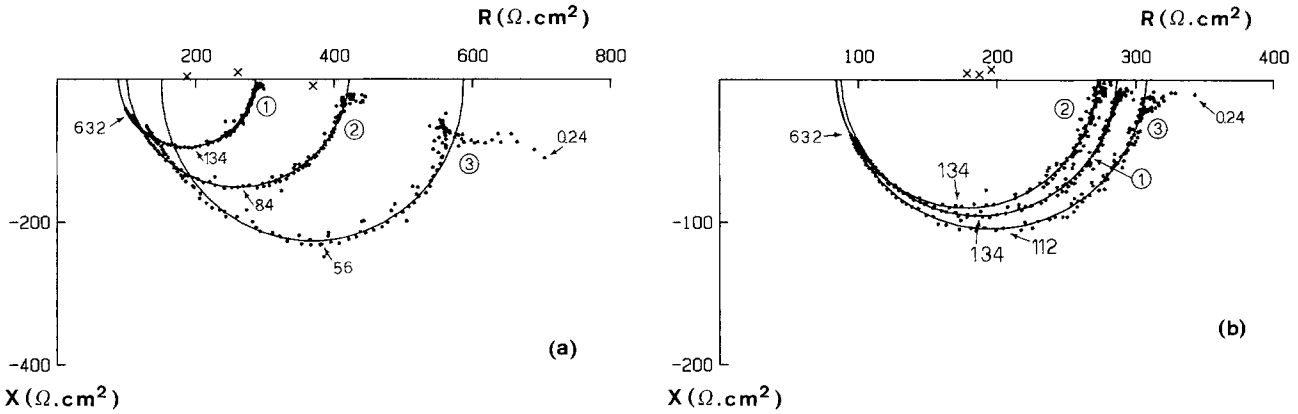

Fig. 2. Impedance loci recorded at mucosa-negative (*a*) and mucosa-positive (*b*) transepithelial clamp potentials. In (*a*) the potential was 0, −18 and −64 mV (curves 1, 2 and 3, respectively), and in (*b*) it was 0, +18 and +64 mV (curves 1, 2 and 3, respectively). The marks(×) indicate the centers of the semicircles that were fitted to the data. The numbers on the semicircles are frequencies in Hz

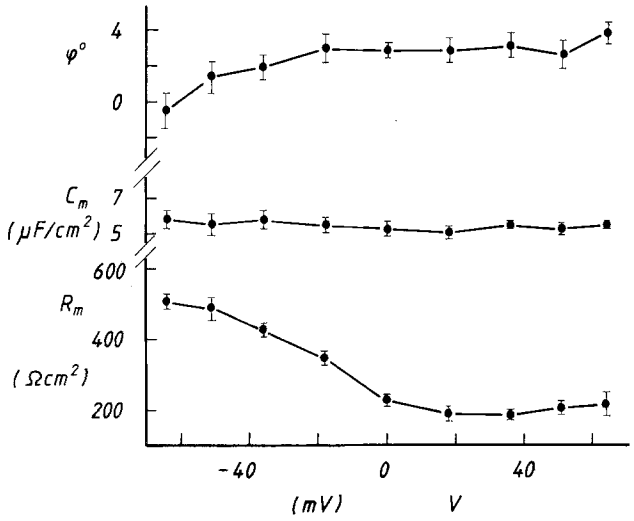

Fig. 3. Equivalent parallel resistance R_m, equivalent parallel capacitance C_m and angle φ as functions of the transepithelial potential V across the preparation. The epithelium was exposed to NaCl-Ringer's + 10 mM TAP on both sides. Number of observations: $N = 9$

(Gögelein & Van Driessche, 1981) the spectra could be well fitted by the sum of a Lorentzian and an A/f^{α} component in the low- and middle-frequency region. However, at frequencies above 10 Hz the data points deviated significantly from the fitted curve (Fig. 4*b*). Therefore spectral values above 10 Hz were excluded from the fitting procedure (indicated by arrows in Fig. 4). The plateau values and corner frequencies of seven experiments are summarized in Table 1 (row 1). Clamping the epithelium at negative potentials increased the amplitudes of the spectral values over the entire frequency range. However, the increase is most pronounced in the middle frequency range, so that the Lorentzian component became more apparent. In the example demonstrated in Fig. 4*a*, a Lorentzian could not be fitted to the data at zero clamp potential. However, at −18 mV a Lorentzian component became clearly visible. In the low- and middle-frequency range the data points could be fitted by the sum of a Lorentzian and an A/f^{α} component, but they departed from this curve at frequencies above 20 Hz. Therefore these points were excluded from the fits. The plateau values and corner frequencies thus obtained are summarized in Table 1 (row 2). The data show that S_o increased but that f_c did not change significantly, compared to the values obtained at zero potential. Increasing the potential to −36 mV enhanced the spectral values further and produced 'peaking' of the plateau in 5 of 12 bladders (not shown). In all cases where peaking of the plateau was observed, the impedance locus showed a pronounced LF capacitive feature. On the other hand, peaking in the power spectra was unimpressive when the LF component in the impedance function was only weakly visible. Power spectra with peaking were not fitted. In the seven cases where no peaking was apparent the spectra could be fitted in most cases solely by a Lorentzian. Mean values of S_0 and f_c (Table 1, row 3) demonstrate only a slight increase of S_o and no appreciable change of f_c, compared to data obtained at −18 mV. Increasing the potential further to −51 and −64 mV increased the spectral values only slightly but produced pronounced peaking (Fig. 4*a*). In all cases the corresponding impedance locus showed a marked capacitive as well as inductive LF feature. When the epithelium was clamped at −64 mV (Fig. 4*a*), the slope of the spectrum in the the high frequency range is close to −2, the value expected for a Lorentzian curve.

The relaxation noise component, enhanced by negative potentials was abolished by the addition of 5 mM TEA^+ to the mucosal side. At $V = -64$ mV, the Lorentzian component, showing pronounced

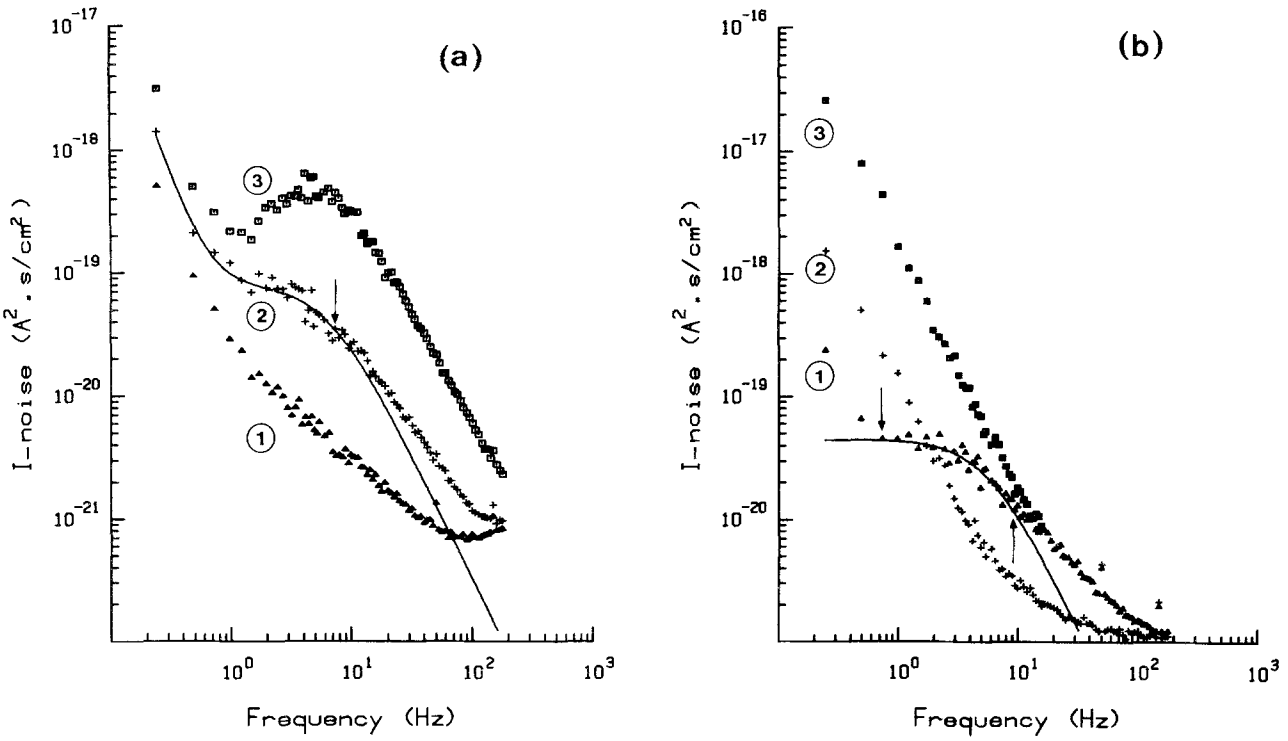

Fig. 4. Effect of mucosa-negative (*a*) and mucosa-positive (*b*) transepithelial clamp potentials on power spectra of current noise. In (*a*) the potential was 0, −18 and −64 mV (spectra 1, 2 and 3, respectively). In (*b*) the epithelium was clamped at 0, +36 and +64 mV (spectra 1, 2 and 3, respectively). The arrows demarcate data points, that were used to fit the spectra

peaking, disappeared after application of TEA^+, so that only an A/f^α noise component remained. In the impedance loci, the inductive as well as capacitive LF features vanished with TEA^+ (Gögelein & Van Driessche, 1980). The inhibition of the relaxation noise component by TEA^+ provides additional evidence that the fluctuations, enhanced by negative potentials, are due to conductance fluctuations of apical K^+ channels.

Fig. 4*b* illustrates the influence of a mucosa-positive potential on current fluctuations. In this experiment a relaxation noise component was obtained at zero potential. Clamping the epithelium at 18 mV decreased this noise component to such an extent that the data could not be fitted by a Lorentzian (for clarity not shown in Fig. 4*b*). When the voltage was raised to 36 mV, the spectral values decreased further in the middle frequency range, but concomitantly the LF noise component increased (Fig. 4*b*, curve 2). With further increasing potential the spectral values increased over the entire frequency range. As demonstrated in Fig. 4*b* (curve 3), the spectral values at $V=64$ mV exceed those obtained at $V=0$ mV in the low- and middle-frequency range. The power spectrum yields an A/f^α component, with α being about 2.

In a few cases voltage noise was recorded under current-clamp conditions immediately after the measurement of current noise spectra at −64 mV. A constant current was adjusted under current clamp, so that a transepithelial voltage of −64 mV was achieved. Fig. 5 shows typical power density spectra of current and voltage noise together with the magnitude of the impedance. Peaking is pronounced in the current-noise spectrum but is only weakly visible in the spectrum of voltage-noise. The steep decline of the slope of the voltage noise spectrum presumably reflects the decline of $|Z|$ at frequencies above 30 Hz.

So far these results confirm our previous finding that the relaxation noise component, observed under control conditions, is due to a K^+ efflux through the apical membrane. Transepithelial voltages are able to reduce or to augment this K^+ efflux, which

Table 1. Plateau value S_o and corner frequency f_c at different transepithelial clamp potentials

Clamp potential (mV)	S_o (A^2 sec/cm^2)	f_c (Hz)	N
$V=0$	$(1.8\pm0.5)\times10^{-20}$	8.6±1.1	7
$V=18$	$(9.2\pm0.2)\times10^{-20}$	8.6±0.6	8
$V=-36$	$(1.6\pm0.4)\times10^{-19}$	7.8±1.1	7

Solution on both sides: NaCl-Ringer's + 10 mM TAP.
N = number of observations

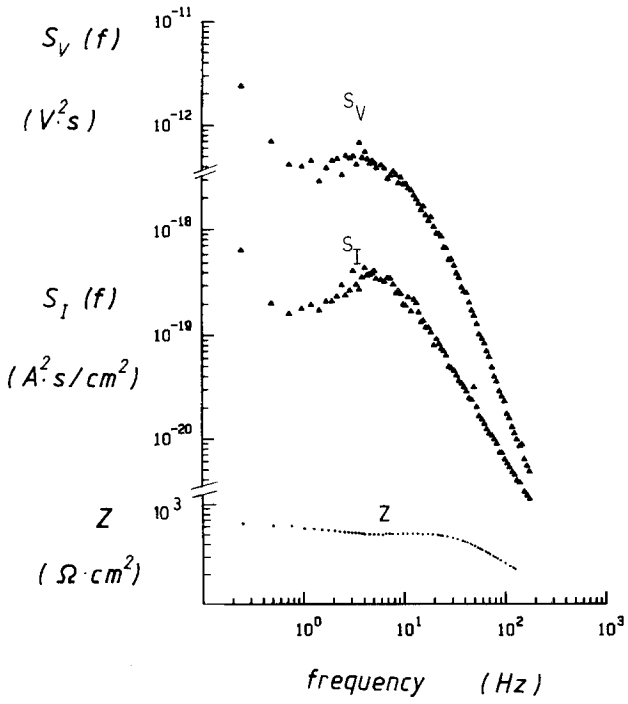

Fig. 5. Power spectra of voltage noise $S_V(f)$ and current noise $S_I(f)$, as well as the magnitude of the impedance Z of a *Necturus* gallbladder, exposed to NaCl-Ringer's (+10 mM TAP) on both sides. The transepithelial potential was −64 mV in all cases

is expressed in a decrease or increase of the plateau of the relaxation noise component.

Fluctuations with KCl-Ringer's on the Serosal Side

Previously we reported (Van Driessche & Gögelein, 1978; Gögelein & Van Driessche, 1981) that K^+ relaxation noise increased considerably when all Na^+ was replaced by K^+ on the serosal side. It was concluded that this increase is due to an increased transcellular K^+ flow, directed from the serosal to the mucosal side of the epithelium. A mucosa-negative potential is expected to enhance this K^+ flux and therefore the relaxation noise component should increase. On the other hand, a positive potential should counteract this K^+ flux and consequently the K^+ relaxation noise should decrease. Fig. 6*a* demonstrates the effect of increasing negativity on current noise spectra. Spectrum 1 was recorded by clamping at the uncorrected biionic potential. As discussed in the preceding paper, the data points could be fitted by the sum of a Lorentzian and an A/f^α component in the low- and middle-frequency range, but they departed from the fitted curve at frequencies above 10 Hz. Similar to the results obtained with NaCl-Ringer's on both sides, the relaxation noise as well

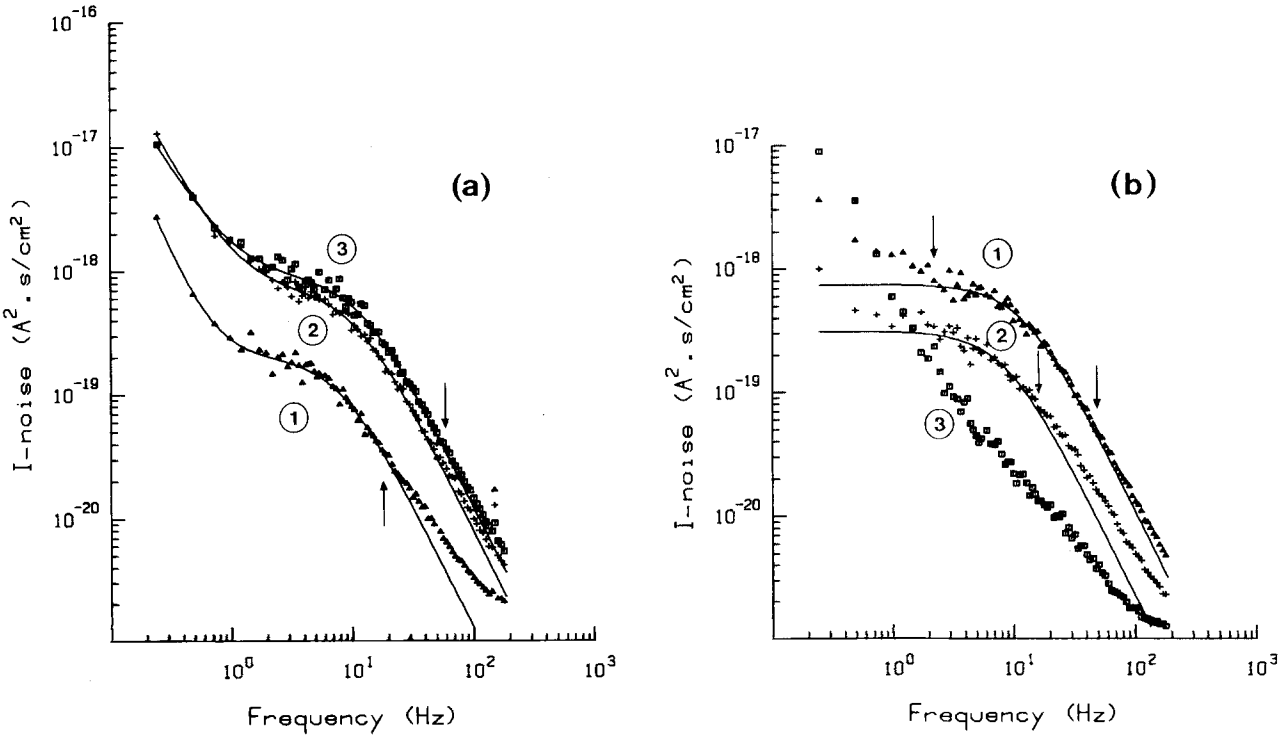

Fig. 6. Effect of negative (*a*) and positive (*b*) transepithelial potentials on the power spectra of current fluctuations. The epithelium was exposed to KCl-Ringer's on the serosal and to NaCl-Ringer's on the mucosal side (+10 mM TAP on both sides). In (*a*) the potential was +8.7 mV (=uncorrected biionic potential), −18 and −36 mV (curves 1, 2 and 3, respectively). In (*b*) the potential was +8.3, +18 and +36 mV (curves 1, 2 and 3, respectively)

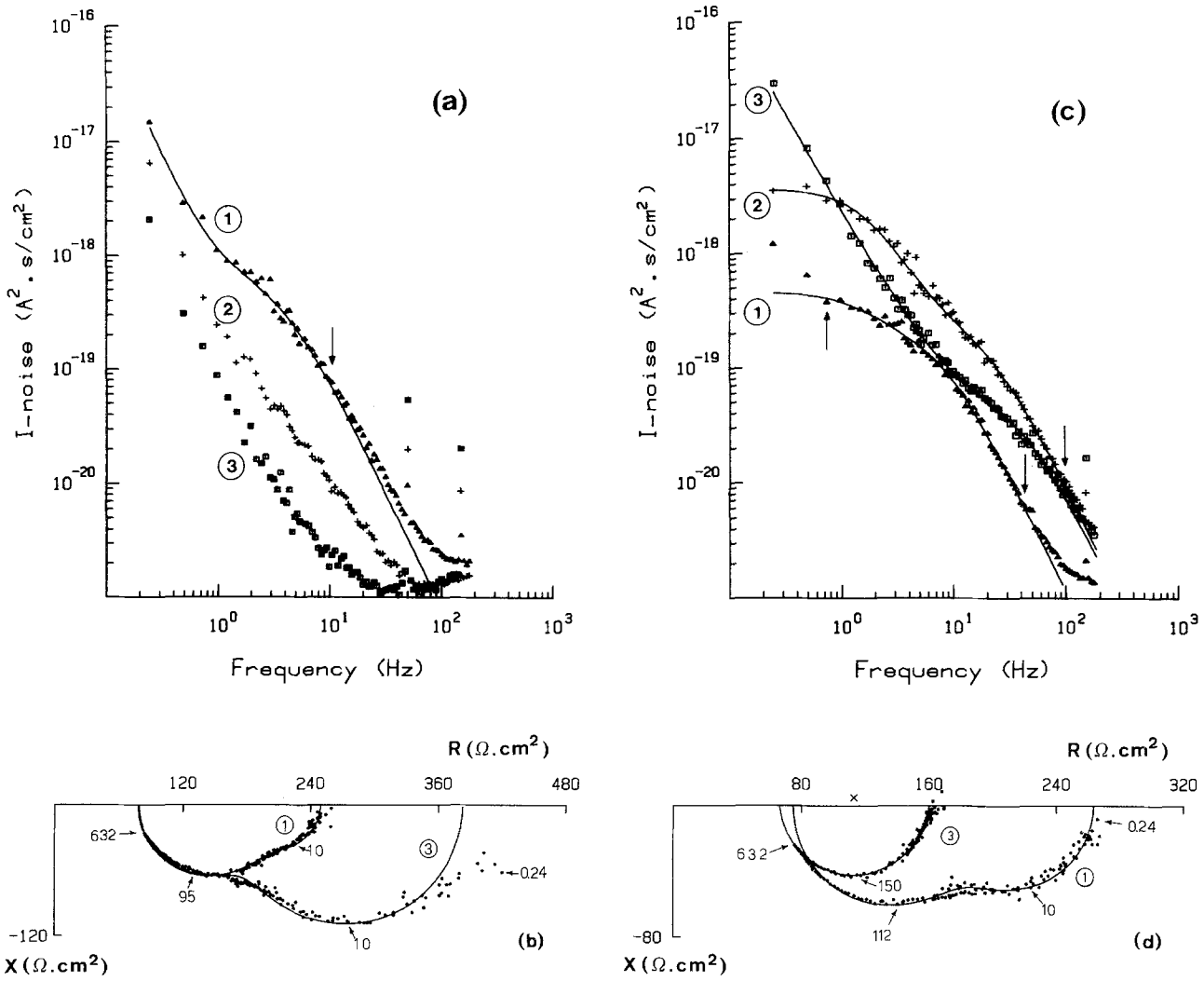

Fig. 7. Effect of negative and positive potentials on power spectra and impedance loci of *Necturus* gallbladder, exposed to KCl-Ringer's on the mucosal and NaCl-Ringer's on the serosal side (+10 mM TAP on both sides). (*a*) The potential was −9.1 mV (uncorrected biionic potential), −36 and −64 mV (spectra 1, 2 and 3, respectively). (*b*) Impedance loci corresponding to power spectra of (*a*). They were fitted by the function given by Eq. (6). The numbers near the impedance loci are frequencies in Hz. (*c*) The potential was −7.7, +18 and +51 mV (spectra 1, 2 and 3, respectively). Spectra 1 and 2 were fitted by two superimposed Lorentzians. (*d*) Impedance loci that correspond to spectra in (*c*). Curve 1 was fitted by the function of Eq. (6), whereas curve 3 was fitted by a semicircle. The mark (×) near the real axis is the center of this semicircle

as the LF noise component increased with increasing negativity. Clamping at −18 mV increased S_o from $(1.5\pm0.4)\ 10^{-19}$ A²sec/cm² (zero current flow) to $(4.7\pm1.1)\ 10^{-19}$ A²sec/cm² and increased f_c from (7.7 ± 0.6) Hz to (10.5 ± 0.7) Hz ($N=4$). It is interesting to note that the data points deviate from the fitted curve only at frequencies above 50 Hz (curve 2). Clamping at −36 mV enhanced the relaxation noise component only slightly (curve 3). In spectra having less intense LF noise than the one shown in Fig. 6*a*, peaking became apparent at this potential. Clamping at −51 and −64 mV did not increase the spectral values in the middle-frequency range but produced pronounced peaking of the plateau (not shown). A capacitive LF component appeared in the impedance locus when peaking in the power spectrum was observed, as in the case with NaCl-Ringer's on both sides.

Typical power spectra obtained with mucosa-positive clamp potentials are illustrated in Fig. 6*b*. Clamping at 18 mV reduced the plateau value of the relaxation noise component, present under zero current flow (curves 2 and 1, respectively). The Lorentzian was depressed to such an extent that fits could not be performed (curve 3) when the potential was raised to 36 mV. On the other hand, the amplitudes of the spectral values in the LF region increased. Increasing the potential to 64 mV caused an increase

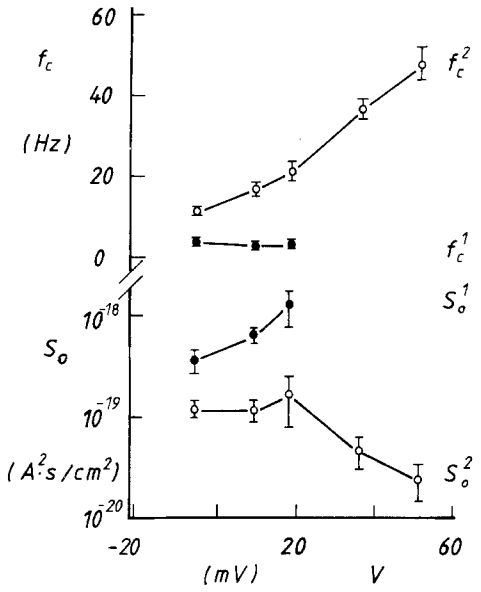

Fig. 8. Plateau values S_o^1 and S_o^2 and corner frequencies f_c^1 and f_c^2 as functions of the transepithelial clamp potential in bladders, exposed to KCl-Ringer's on the mucosal and to NaCl-Ringer's on the serosal side (+10 mM TAP^+ on both sides). Number of observations: $N=6$

of the spectral values in the entire frequency range, so that the power spectrum yielded a straight line, having a slope of about −2 (not shown).

Fluctuations with KCl-Ringer's on the Mucosal Side

Substitution of all Na^+ by K^+ at the mucosal side produced relaxation noise in the gallbladder, which is caused by an influx of K^+ ions from the mucosal bath into the cells (Van Driessche & Gögelein, 1978). Consequently we expect a negative potential to depress this noise type, whereas the noise should be enhanced by a positive potential. The effect of a mucosa-negative potential on current fluctuations is shown in Fig. 7*a*. Curve 1 was recorded under zero current flow and was fitted by the sum of a Lorentzian and an A/f^α component in the low- and middle-frequency range. The data points above 10 Hz could not be fitted by this curve and were excluded from the fitting procedure. Clamping at −18 mV decreased the spectral values in the entire frequency range (not shown). In contrast to spectra recorded at zero current flow, the spectra at −18 mV could be fitted over almost the entire frequency range by the sum of a Lorentzian and an A/f^α component. Besides a slight decrease of the plateau value, the corner frequency increased significantly from (5.8 ±0.5) Hz to (7.4±0.8) Hz ($N=6$, $p<0.01$). At $V=-36$ mV the relaxation noise component was decreased to such an extent that it could not be fitted by a Lorentzian (curve 2). Raising the potential to −64 mV decreased the spectral values further over the entire frequency range (curve 3). Fig. 7*b* demonstrates the corresponding impedance loci at −9.1 mV (curve 1) and −64 mV (curve 3) clamp potential. The data were recorded with method 1. They are fitted with the function given by Eq. (6). As described elsewhere (Gögelein & Van Driessche, 1980) the capacitive LF component is due to a polarization impedance caused by mucosal KCl-Ringer's. Curve 3 shows that with increasing negativity the resistive part of this LF component increases considerably. Mean values of 5 experiments are: $R_d=(72\pm6)\,\Omega cm^2$, $C_d=(152\pm28)\,\mu F/cm^2$ when the epithelium was clamped at the biionic potential and $R_d=(266\pm32)\,\Omega cm^2$ and $C_d=(78\pm14)\,\mu F/cm^2$ when the potential was −64 mV. Under the same conditions the equivalent resistance R_m decreased from $(137\pm11)\,\Omega cm^2$ to $(121\pm16)\,\Omega cm^2$, whereas C_m did not change significantly. C_m was about 7 $\mu F/cm^2$ in all cases.

Fig. 7*c* shows typical power spectra recorded at mucosa-positive potentials when the mucosal side was bathed with KCl-Ringer's (+10 mM TAP^+ on both sides). Spectrum 1 was obtained when the epithelium was clamped at the uncorrected biionic potential. Clamping at 18 mV increased the spectral values over the entire frequency range. Concomitantly two relaxation noise components became clearly visible in the spectrum. These spectra were fitted by two superimposed Lorentzians (curve 2). Because of this observation we assume that at zero current flow the deviation of the data points from a Lorentzian curve at frequencies above 10 Hz is due to the existence of an additional relaxation component. Therefore spectrum 1 in Fig. 7*c* was fitted by the sum of two Lorentzians. Hereafter the left Lorentzian, characterized by the plateau value S_o^1 and the corner frequency f_c^1, is designated as 'slow component', whereas the right Lorentzian is designated as 'fast component' (referred to with index 2). At potentials of 36 and 51 mV the slow component disappeared, whereas the fast one could still be observed. Hence the power spectra could be fitted by the sum of one Lorentzian and an A/f^α component (curve 3). At 64 mV LF noise became dominant and masked all other components (not shown). In Fig. 8 the plateau values and corner frequencies are plotted as a function of the potential. These data demonstrate how S_o^1 increases with positive potentials whereas f_c^1 decreases slightly. S_o^2 does not change up to 18 mV, but decreases significantly at higher potentials, whereas f_c^2 gradually shifted to higher frequencies. After addition of 5 mM TEA^+ to the mucosal side, the fast as well as the slow relaxation noise components vanished at all potentials.

The corresponding impedance loci (Fig. 7*d*) demonstrate that the LF component, present at zero transepithelial current flow (curve 1) vanished at the potential of 51 mV. This means that polarization phenomena, arising at high mucosal K^+ concentration, disappear at high positive potentials. R_m decreased with increasing positively whereas C_m did not change significantly.

Discussion

Impedance Measurements

The mechanism of transepithelial resistance change under d-c current flow could be related to geometrical changes of the paracellular interspaces (Bindslev et al., 1974). The authors demonstrated that the interspaces narrow with serosa-to-mucosa current flow but dilate with current flow in the opposite direction. Transepithelial voltage transients were observed when current steps from mucosa to serosa were applied across the epithelium (Wedner & Diamond, 1969; Bindslev et al., 1974; Reuss & Finn, 1977). Reuss and Finn (1977) showed that these voltage transients are the consequence of changes in the equivalent emf's of the shunt and the cell membranes. The largest emf change (polarization) took place at the basolateral membrane. They concluded that polarization emf's were caused by K^+ concentration changes, mainly at the unstirred layer in contact with the basolateral membrane. The impedance locus of Fig. 2*a* (curve 3) indicates a capacitive element which, in the lumped circuit, can approximately be represented as a parallel combination of a capacitance and a resistance, connected in series to the epithelial equivalent circuit (Fig. 1*b*). This capacitive LF feature probably reflects a polarization phenomena. It can be assumed that it has the same origin as the voltage transients mentioned above.

Fluctuation Analysis with NaCl-Ringer's on Both Sides

The influence of an electrical gradient on current fluctuations under control conditions is consistent with the effect of a chemical K^+ gradient. A K^+ concentration gradient, directed from serosa to mucosa (KCl-Ringer's serosal) increased the relaxation noise, caused by an increased K^+ efflux from the cells into the mucosal medium (Van Driessche & Gögelein, 1978). In this paper we showed that an electrical gradient had a similar effect: A mucosa-negative potential depolarizes the apical cell membrane (Reuss & Finn, 1977) and consequently an increased K^+ efflux into the mucosal solution can be expected. The experiments in Fig. 4*a* confirm this assumption. On the other hand a mucosa-positive potential hyperpolarizes the apical membrane. Consequently a reduction of an existing apical K^+ efflux can be expected. This assumption is supported by the decrease of the Lorentzian noise as shown in Fig. 4*b*. In a similar way, a spontaneous Lorentzian was suppressed by increasing mucosal K^+ concentration to 36 mM (Van Driessche & Gögelein, 1978). It can be assumed that also in this case the K^+ electrochemical gradient across the apical membranes is reduced. At a mucosal K^+ concentration of 57 mM and higher the Lorentzian noise reappeared. We explained this by a K^+ influx across the apical membrane. In a similar way one would expect an apical K^+ influx and a reappearance of the relaxation noise component at high mucosa-positive clamp potentials. This reappearance could not be observed, because of the concomitant increase of LF noise (Fig. 4*b*). As discussed in the preceding paper (Gögelein & Van Driessche, 1981) this LF noise is presumably associated with diffusional flow of ions across the tight junctions as well as across cell membranes.

Model calculations showed that the transepithelially recorded current fluctuations, arising from conductance fluctuations in the apical membrane, were attenuated by resistances and capacitances, being in series or in parallel with the noise source (Van Driessche & Gögelein, 1980). The attenuation decreases with increasing shunt resistance R_p, but increases with increasing series resistance R_s. As demonstrated in Fig. 2*a*, the transepithelial (R_t) as well as the polarization resistance (R_d) increase with increasing negativity. As R_t mainly reflects the resistance of the shunt pathway (Frömter, 1972), and as R_d is in series with the epithelial impedance, the increase of R_t and R_d have opposite effects on the attenuation of the current fluctuations.

Apparent Saturation of the K^+ Channel Current

Comparison of the power spectra in Fig. 4*a* and Fig. 6*a* shows that the increase of the relaxation noise component caused by increasing negativity is more pronounced in experiments with NaCl-Ringer's on both sides than with KCl-Ringer's on the serosal side. In addition, with serosal KCl-Ringer's the spectral values did not increase significantly after raising the potential from -36 to -64 mV. This apparent saturation of the fluctuating K^+ current may have several reasons: (1) The increase of the driving force for K^+ ions at the apical membrane is not proportional to the transepithelial potential because of polarization effects. (2) With increasing negativity the number of fluctuating pores

decreases, due to a voltage dependent 'gating' of the channels. (3) The single-channel current increases only subproportionally with the driving force because of saturation of the transport rate of the single channels. With the available data it is not possible to decide which of these effects causes the apparent saturation of the amplitude of the relaxation noise component.

Evidence for Two Types of K^+ Channels

With KCl-Ringer's on the mucosal side two Lorentzians became evident at positive clamp potentials (Fig. 7*c*). The corresponding impedance function demonstrates that the existing LF capacitive component, present at zero current flow (Fig. 7*d*, curve 1) vanished at a clamp potential of 51 mV (curve 3). Consequently, the power spectrum cannot be influenced by a series impedance and therefore frequency-dependent attenuation effects arising from polarization impedances can be excluded. Model calculations showed that the capacitive LF impedance observed at -7.7 mV has no significant frequency-dependent effect on the plateau value of the corresponding power spectrum. However, the series resistance R_s, being about $80\,\Omega cm^2$, attenuates the spectral values over the entire frequency range by a factor of about 5. It seems likely that power spectra, recorded at zero current flow, consisted already of two relaxation noise components, which appeared more clearly with positive potentials. This assumption is supported by the fact that the data points above 10 Hz deviate significantly from a Lorentzian in the spectrum, recorded at zero current flow. In addition, the spectrum could be adequately fitted by two superimposed Lorentzians. One can speculate that the deviation of the spectral values from a Lorentzian curve above 10 Hz, observed with NaCl-Ringer's on both sides as well as with serosal KCl-Ringer's is also due to the existence of an additional Lorentzian component. In the preceding paper (Gögelein & Van Driessche, 1981) wer reported that under these conditions, power spectra could be fitted adequately by the sum of two Lorentzians. This means either that the fluctuating channels have more than one conductance state or that there exist different types of K^+ channels, having open-close kinetics with different relaxation times. In the following section arguments are given which favor the latter possibility.

The Influence of Clamp Potentials on Gating Properties

In this paper it is shown that with KCl-Ringer's on the serosal side the corner frequency increased with increasing negative clamp potential (Fig. 6*a*). Under these conditions a K^+ flux from the cell interior into the mucosal solution is enhanced. On the other hand, f_c decreased with increasing K^+ flux from the mucosal side into the cell. This was achieved by increasing positive potentials, when KCl-Ringer's was on the mucosal side (Fig. 7*c*). This indicates that the relaxation time of the open-close process of these K^+ channels depends on the direction of electrically induced K^+ flow. The corner frequency of the fast process, however, behaved in the opposite way: it increased strongly at positive potentials with mucosal KCl-Ringer's (Fig. 7*c*), whereas it disappeared at negative potentials with serosal KCl-Ringer's (Fig. 6*a*). A tentative explanation of these findings would be the existence of two types of K^+ channels in the apical membrane which have different relaxation times and behave differently to transmembrane K^+ flow.

The Effect of Peaking in Power Spectra

In all cases where peaking of the plateau was observed, the impedance locus had a capacitive as well as an inductive LF component (Fig. 2*a*). Inductive LF features alone, as observed with KCl-Ringer's on the serosal side (at zero current flow) (Gögelein & Van Driessche, 1980) did not cause peaking in power spectra. Such inductive LF features can be represented as a parallel combination of an inductance and a resistance, connected in series to the epithelial equivalent network (*to be published*). Model calculations showed that such inductive series impedances do not produce pronounced peaking in power spectra (*unpublished results*). However, calculations demonstrated that a parallel combination of a resistance R_d and a capacitance C_d, connected in series with the equivalent epithelial circuit (Fig. 1*b*) attenuates an excess noise signal more intensely in the low- than in the high-frequency region (Van Driessche & Gögelein, 1980). The attenuated power spectrum for white excess noise is constant both at low and high frequencies but declines from the high- to the low-frequency range. The frequency where this transition occurs is in the order of magnitude of the characteristic frequency $f_0 = 1/(2 \cdot \pi \cdot R_d \cdot C_d)$ of the polarization impedance. With NaCl-Ringer's on both sides and at high negative potentials f_0 of the LF impedance is estimated from impedance loci to be in the order of 1 Hz. If the intrinsic noise spectrum has a Lorentzian shape, the transepithelially recorded spectrum, which is attenuated by the polarization impedance, will reach a plateau at frequencies well below f_o. Due to the decline of the attenuation, spectral values will increase in the frequency

range around f_o. As the spectral values of a Lorentzian curve decline with the slope -2 at frequencies above the corner frequency, the spectrum will show a peak. However, at low frequencies this 'peaked' Lorentzian overlaps with LF noise (Fig. 4*a*, curve 3). Since exact estimations of the equivalent parameters R_d and C_d are not possible from the recorded impedance loci, no corrections of the individual power spectra were performed. In addition, the model calculations demonstrated that the polarization impedance has no effect on the frequency dependence of the voltage noise. Consequently, the voltage power spectra should show no peaking if the intrinsic conductance fluctuations are of Lorentzian type. The experiment of Fig. 5 demonstrates that peaking is only weakly visible in voltage noise spectra, whereas it is pronounced in the corresponding current noise spectrum. The peaking in the voltage noise spectrum may be due to the fact that (1) the equivalent representation of the polarization effect as an RC network in series to the epithelial network is only an approximation (Sandblom, Walker & Eisenman, 1972), or (2) that the spectra of the intrinsic conductance fluctuations show already slight peaking under these experimental conditions (Chen, 1975, 1978).

The authors would like to thank Dr. T. Hoshiko for critical reading of the manuscript and for revising the English.

References

Bindslev, N., Tormey, J.McD., Wright, E.M. 1974. The effects of electrical and osmotic gradients on lateral intercellular spaces and membrane conductance in a low resistance epithelium. *J. Membrane Biol.* **19**:357

Chen, Y. 1975. Fluctuations and noise in kinetic systems. III. Cycling steady-state models. *J. Theor. Biol.* **55**:229

Chen, Y. 1978. Differentiation between equilibrium and non-equilibrium kinetic systems by noise analysis. *Biophys. J.* **21**:279

Clausen, C., Lewis, S.A., Diamond, J.M. 1979. Impedance analysis of a tight epithelium using a distributed resistance model. *Biophys. J.* **26**:291

Cole, K.S., Cole, R.H. 1941. Dispersion and adsorption in dielectrics. I. Alternating current characteristics. *J. Chem. Phys.* **9**:341

Frömter, E. 1972. The route of passive ion movement through the epithelium of *Necturus* gallbladder. *J. Membrane Biol.* **8**:259

Gögelein, H., Hegel, U., Weskamp, P. 1975. Influence of DC current flow on electrical impedance of *Necturus* gall bladder epithelium. *Pfluegers Arch.* **359**:R126

Gögelein, H., Van Driessche, W. 1979. Noise analysis in *Necturus* gallbladder, estimation of single channel conductance and the effect of an electrical gradient. *Pfluegers Arch.* **379**:R30

Gögelein, H., Van Driessche, W. 1980. Low frequency impedance of *Necturus* gallbladder. *Proc. Int. Union Physiol. Sci.* **14**:442

Gögelein, H., Van Driessche, W. 1981. Noise analysis of the K^+ current through the apical membrane of *Necturus* gallbladder. *J. Membrane Biol.* **60**:187

Lindemann, B., Van Driessche, W. 1977. Sodium-specific membrane channels of frog skin are pores: Current fluctuations reveal high turn-over. *Science* **195**:292

Reuss, L., Finn, A.L. 1977. Mechanisms of voltage transients during current clamp in *Necturus* gallbladder. *J. Membrane Biol.* **37**:299

Reuss, L., Weinman, S.A. 1979. Intracellular ionic activities and transmembrane electrochemical potential differences in gallbladder epithelium. *J. Membrane Biol.* **49**:345

Sandblom, J., Walker, J.L., Eisenman, G. 1972. The transient response and impedance locus of a mobile site membrane. *Biophys. J.* **12**:587

Schifferdecker, E., Frömter, E. 1978. The AC impedance of *Necturus* gallbladder epithelium. *Pfluegers Arch.* **377**:125

Van Driessche, W., Gögelein, H. 1978. Potassium channels in the apical membrane of the toad gallbladder. *Nature (London)* **275**:665

Van Driessche, W., Gögelein, H. 1980. Attenuation of current and voltage noise signals recorded from epithelia. *J. Theor. Biol.* **86**:629

Van Driessche, W., Lindemann, B. 1978. Low-noise amplification of voltage and current fluctuations arising in epithelia. *Rev. Sci. Instrum.* **49**:52

Van Driessche, W., Zeiske, W. 1980*a*. Spontaneous fluctuations of potassium channels in the apical membrane of frog skin. *J. Physiol. (London)* **299**:101

Van Driessche, W., Zeiske, W. 1980*b*. Ba^{2+}-induced conductance fluctuations of spontaneously fluctuating K^+ channels in the apical membrane of frog skin (*Rana temporaria*). *J. Membrane Biol.* **56**:31

Verveen, A.A., Felice, L.J. de 1974. Membrane noise. *Prog. Biophys. Mol. Biol.* **28**:189

Wedner, H.J., Diamond, J.M. 1969. Contributions of unstirred-layer effects to apparent electrokinetic phenomena in the gallbladder. *J. Membrane Biol.* **1**:92

Zeuthen, T. 1978. Intercellular gradients of ion activities in the epithelial cells of the *Necturus* gallbladder recorded with ion-selective microelectrodes. *J. Membrane Biol.* **39**:185

Received 21 April 1980; revised 30 October 1980, 2 January 1981